

See discussions, stats, and author profiles for this publication at: <https://www.researchgate.net/publication/5670654>

# Characterization of NAD Uptake in Mammalian Cells

Article in *Journal of Biological Chemistry* · April 2008

DOI: 10.1074/jbc.M706204200 · Source: PubMed

CITATIONS

52

READS

55

9 authors, including:



**Richard Billington**

University of Plymouth

38 PUBLICATIONS 1,471 CITATIONS

SEE PROFILE



**Emanuela Ercolano**

University of Plymouth

23 PUBLICATIONS 518 CITATIONS

SEE PROFILE



**Cristina Travelli**

Amedeo Avogadro University of Eastern Piedmont

23 PUBLICATIONS 390 CITATIONS

SEE PROFILE



**Ambra A Grolla**

Amedeo Avogadro University of Eastern Piedmont

26 PUBLICATIONS 433 CITATIONS

SEE PROFILE

Some of the authors of this publication are also working on these related projects:



StarTrEgg [View project](#)



NAADP binding [View project](#)

# Characterization of NAD Uptake in Mammalian Cells\*

Received for publication, July 27, 2007, and in revised form, January 4, 2008. Published, JBC Papers in Press, January 7, 2008, DOI 10.1074/jbc.M706204200

Richard A. Billington<sup>1</sup>, Cristina Travelli, Emanuela Ercolano, Ubaldina Galli, Cintia Blasi Roman, Ambra A. Grolla, Pier Luigi Canonico, Fabrizio Condorelli, and Armando A. Genazzani

From the Dipartimento di Scienze Chimiche, Alimentari, Farmaceutiche e Farmacologiche and the Drug and Food Biotechnology Center, Università del Piemonte Orientale, Via Bovio 6, Novara 28100, Italy

Recent evidence has shown that NAD(P) plays a variety of roles in cell-signaling processes. Surprisingly, the presence of NAD(P) utilizing ectoenzymes suggests that NAD(P) is present extracellularly. Indeed, nanomolar concentrations of NAD have been found in plasma and other body fluids. Although very high concentrations of NAD have been shown to enter cells, it is not known whether lower, more physiological concentrations are able to be taken up. Here we show that two mammalian cell types are able to transport low NAD concentrations effectively. Furthermore, extracellular application of NAD was able to counteract FK866-induced cell death and restore intracellular NAD(P) levels. We propose that NAD uptake may play a role in physiological NAD homeostasis.

Pyridine nucleotides, although often considered as simple redox cofactors in the cell, are in fact multifunctional molecules involved in a wide range of cellular processes (1). It is becoming clear that NAD(P) is involved in more pharmacologically attractive cellular processes such as cell signaling, transcriptional regulation, and post-translational protein modification (2, 3). For example, NAD(P) has been shown to be the precursor of molecules involved in calcium signaling (e.g. cADPR,<sup>2</sup> NAADP, and ADPR), to be involved in the regulation of epigenetic changes via sirtuins and to be a substrate for both mono- and poly-ADP-ribosylation (3–5).

The general perception is that cellular NAD is synthesized either *de novo* from tryptophan or via one of two possible recycling pathways: from nicotinic acid or nicotinamide (together referred to as vitamin PP, or niacin) (6). Recently, a third biosynthesis pathway has been described, which uses nicotinamide riboside as a precursor (7).

The presence of membrane-bound ectoenzymes that use NAD(P) (8) has led to the investigation and description of several mechanisms for the export of NAD across the plasma

membrane, including transport through connexins and stimulus-induced exocytotic release (9–11). Surprisingly, though, the possibility that low NAD concentrations can be imported across the membrane to directly replenish the cellular NAD(P) pools bypassing biosynthetic pathways has not been conclusively addressed. However, circumstantial evidence suggests that this may occur: (i) High concentrations of extracellularly applied NAD(H) have been shown to increase intracellular NAD levels (10, 12–14); (ii) extracellular NAD counteracts PARP-induced intracellular NAD depletion (12, 15); (iii) CD38 knock-out mice, which are impaired in their ability to degrade extracellular NAD, display higher endogenous SIRT1 activity (16); (iv) uptake processes have been shown for the Ca<sup>2+</sup>-mobilizing NAD(P) metabolites cADPR and NAADP in a variety of diverse mammalian cell types (17–21); (v) NAD and at least one of the enzymes involved in biosynthesis are present extracellularly (13, 22, 23); and (vi) Wallerian degeneration can be slowed by the addition of extracellular NAD (24).

Here we show that various mammalian cell types are able to transport picomolar concentrations of NAD across the plasma membrane from the extracellular medium. When intracellular NAD(P) levels were reduced by treatment with the NAD biosynthesis inhibitor FK866 (APO866, (*E*)-*N*-[4-(1-benzoylpiperidin-4-yl)butyl]-3-(pyridin-3-yl)acrylamide (25)), application of NAD extracellularly was able to partially replenish these levels. Furthermore, cells could be rescued from FK866-induced NAD depletion, autophagy, and cell death by addition of NAD to the culture medium. These data, taken together, suggest that NAD uptake can participate in the homeostasis of cellular NAD levels.

## EXPERIMENTAL PROCEDURES

**Cell Culture**—NIH-3T3 murine epithelial cells were cultured in RPMI 1640 (Sigma) supplemented with 5% FBS (fetal bovine serum), 2 mM glutamine, 10 units/ml penicillin, and 100 µg/ml streptomycin. SH-SY 5Y cells were cultured in Dulbecco's modified Eagle's medium (Sigma) supplemented with 10% fetal bovine serum, 2 mM glutamine, 10 units/ml penicillin, and 100 µg/ml streptomycin. HMEC, HeLa, HaCaT, K562, and RAW 264.7 cells were cultured according to the conditions suggested by the ATCC. Cells were maintained in a humidified incubator supplied with 5% CO<sub>2</sub>/95% air at 37 °C and were subcultured as needed by detaching the cells with 0.25% trypsin and 5 mM EDTA.

**[<sup>32</sup>P]NAD Transport**—Cells plated in 6-well plates were grown to confluence. The wells were washed twice with 1 ml of warm Locke buffer (134 mM NaCl, 4 mM NaHCO<sub>3</sub>, 5 mM KCl, 2.3 mM CaCl<sub>2</sub>, 10 mM HEPES, 1 mM MgCl<sub>2</sub>, 5 mM glucose, pH 7.4) before addition of 0.5 ml of Locke buffer or modifications thereof (NMG Locke contained 134 mM *N*-methylglucamine in

\* The costs of publication of this article were defrayed in part by the payment of page charges. This article must therefore be hereby marked "advertisement" in accordance with 18 U.S.C. Section 1734 solely to indicate this fact.

<sup>1</sup> To whom correspondence should be addressed. Tel.: 39-032-137-5835; Fax: 39-032-137-5821; E-mail: billington@pharm.unipmn.it.

<sup>2</sup> The abbreviations used are: ADPR, ADP-ribose; cADPR, cyclic ADPR; NAADP, nicotinic acid adenine dinucleotide phosphate; FK866, (*E*)-*N*-[4-(1-benzoylpiperidin-4-yl)butyl]-3-(pyridin-3-yl)acrylamide; HPLC, high-performance liquid chromatography; MTT, 3-(4,5-dimethylthiazol-2-yl)-2,5-diphenyltetrazolium bromide; EYFP, enhanced yellow fluorescent protein; AIF, apoptosis-inducing factor; PBS, phosphate-buffered saline; cyt-*c*, cytochrome *c*; DPR, dipyrindamole; NMPRTase, nicotinamide phosphoribosyltransferase; LC3, microtubule-associated protein light chain 3; NMG, *N*-methylglucamine.

## NAD Uptake

place of the NaCl (4 mM final Na<sup>+</sup>); EGTA Locke lacked CaCl<sub>2</sub> with the addition of 500 μM EGTA). The reaction was started by the addition of 250 pM [<sup>32</sup>P]NAD (800 Ci/mmol, PerkinElmer Life Sciences) or 250 pM [<sup>32</sup>P]NAADP prepared as described previously (26). Competing compounds and drugs were added to the wells before [<sup>32</sup>P]NAD unless stated in the text. After 10 min (except where indicated), the reaction was stopped by aspiration of the buffer, and the cells were washed twice with 1 ml of Locke buffer. The cells were then dissolved in 1 ml of 0.5 M NaOH. 2 ml of scintillation fluid was added, and the radioactivity associated with the cells was counted using a standard scintillation counting procedure for <sup>32</sup>P. For HPLC analysis of transported NAD, cells were scraped after transport experiments in ddH<sub>2</sub>O, extracted by adding an equal volume of chloroform and run on HPLC as described previously (27).

**Cell Viability Assay**—To analyze cell viability, the colorimetric 3-(4,5-dimethylthiazol-2-yl)-2,5-diphenyltetrazolium bromide (MTT) assay was used. Briefly, cells were plated in 24-well plates and treated as indicated for the appropriate time. FK866 (dissolved in Me<sub>2</sub>SO), and the vehicle control were added to the cells to give a final Me<sub>2</sub>SO concentration no greater than 0.5%. Cells were washed once in Locke buffer and 300 μl of MTT (250 μg/ml in Locke buffer) was added before returning the cells to the incubator for 1 h to allow the formation of the purple formazan crystals. After 1 h, 600 μl of isopropanol/0.1 M HCl was added to each well, and the absorbance was read at 570 nm in a plate reader (Victor<sup>3</sup>V, PerkinElmer Life Sciences).

Alternatively, cell counts were performed. Briefly, cells were detached from the wells by trypsinization, stained with trypan blue to exclude dead cells, and counted in a Bürker Chamber.

**NAD(P) Cycling Assay**—Total cellular NAD(P) was measured using an adaptation of the method described by Gasser *et al.* (28). Cells, grown and treated in 24-well plates, were scraped with the piston of a 1-ml syringe in 100 μl of ddH<sub>2</sub>O on ice, and were extracted with 1 volume of HClO<sub>4</sub> (2 M) for 45 min on ice. The samples were then centrifuged for 1 min at 13,000 × *g*, and the supernatant was diluted with an equal volume of K<sub>2</sub>CO<sub>3</sub> (1 M). After a further 45-min incubation on ice, the insoluble potassium perchlorate was removed by centrifugation for 1 min at 13,000 × *g*. The final pH of the supernatant was 8–8.5. In a black 96-well plate (OptiPlate<sup>TM</sup>-96 F; PerkinElmer Life Sciences) 60 μl of cycling mix was added to 100 μl of the extracted NAD(P). The cycling mix (60 μl) consisted of: 20 μl of 500 mM NaH<sub>2</sub>PO<sub>4</sub>, pH 8.0, 2 μl of 5 mg/ml bovine serum albumin, 0.1 μl of 10 mM resazurin (prepared fresh), 5 μl of 100 mM glucose 6-phosphate (G8404, Sigma), 15 μl of 1 mg/ml glucose-6-phosphate dehydrogenase, 15 μl of purified dihydrolipoyl dehydrogenase (EC 1.8.1.4) (see below). Fluorescence (excitation 544 nm, emission 590 nm) was measured for each well using a plate reader (Victor<sup>3</sup>V, PerkinElmer Life Sciences). Standard curves were generated with authentic NAD subjected to mock extractions were used to generate calibration curves.

The diaphorase was purified as follows: 100 μl of enzyme solution (diaphorase, 12 mg/ml, in 50 mM NaH<sub>2</sub>PO<sub>4</sub>, pH 8.0 adjusted with NaOH) was mixed with 200 μl of bovine serum albumin (5 mg/ml in water) and 1.2 ml of a suspension (2% w/v) of activated charcoal in 50 mM NaCl, 20 mM NaH<sub>2</sub>PO<sub>4</sub>, pH 8.0. After incubation at 37 °C for 30 min, the charcoal was removed

by centrifugation (11,000 × *g*, 10 min, 4 °C), and the supernatant was used directly for the cycling assay.

To ensure that FK866, as an antagonist of an NAD-using enzyme, did not directly affect the enzymes of the cycling assay, calibration curves were performed in the presence and absence of 100 nM and 10 μM FK866. The calibration curves were not affected by the presence of FK866 (data not shown). Furthermore, the assay was not affected by nicotinamide mononucleotide at 100 μM.

**FK866**—FK866 was synthesized using a shorter route with respect to that reported (29) (5 synthetic steps *versus* 7 synthetic steps). In brief, the commercially available 4-piperidine butyric acid hydrochloride was reduced to the corresponding alcohol using lithium aluminum hydride and then chemoselectively *N*-benzoylated. The product was then transformed into an azide using the diphenyl phosphoryl azide/1,8-diazabicyclo[5,4,0]undec-7-ene, sodium azide protocol. Finally, the Staudinger azide-amine reduction gave the amine. This compound was subsequently coupled with (*E*)-3-(3-pyridinyl)-2-propenylchloride (prepared starting from the corresponding carboxylic acid using oxalyl chloride) to give FK866 (overall yield over five steps: 11%). The identity of the product was confirmed by NMR (<sup>1</sup>H and <sup>13</sup>C) and mass spectrometry.

**EYFP-LC3-β Translocation**—Exponentially growing cells were transfected with pEYFP-LC3-β (kind gift of Prof. Jäättelä, Institute of Cancer Biology, Copenhagen, Denmark) by liposome transfection (Lipofectamine 2000, Invitrogen) and seeded 1 day after the transfection on glass chamber slides. After the indicated treatments, the percentage of green cells (a minimum of 100 cells/sample) with green vacuoles (EYFP-LC3-β translocated from cytosol to autophagic vacuoles) was counted using a Leica TCS-SP2 Laser-scanning microscope. For the morphological evaluation of autophagic vacuoles and lysosome co-localization, the acidic compartment of cells was counterstained by labeling the cells by adding 50 nM of LysoTracker red (Molecular Probes) for 1 min at 37 °C to cell culture media immediately before confocal analysis.

**Cytochrome *c* and AIF Immunolocalization**—Cells were grown on 18-mm coverslips and incubated at 37 °C in the presence of the specified compounds. Cells were fixed in PBS containing 4% paraformaldehyde for 15 min at room temperature, washed with PBS, then permeabilized in PBS containing 0.2% Triton X-100 for 5 min. Cells were washed and then incubated with an anti-cyt-*c* antibody (1:500, BD Biosciences) or with anti-AIF (1:250, Sigma-Aldrich) antibody in PBS for 1 h at 37 °C. After washing, cells were stained with an AlexaFluor488-conjugated donkey anti-mouse-IgG (1:250, Molecular Probes, Eugene, OR) in PBS for 1 h at 37 °C. Coverslips were inverted and adhered to the glass slides using a mounting solution (DakoCytomation). Images from fluorescence patterns of the cells were obtained using a Leica TCS-SP2 microscope.

**Apoptotic Nuclei Staining**—For confocal-microscopy analysis of DNA integrity and AIF nuclear localization counterstaining, neuroblastoma cells were plated on 12-mm glass coverslips and maintained for appropriate length of time with different compounds. DRAQ5 (Biostatus Ltd., Leicestershire, UK) DNA dye was used for nuclear staining of living and apoptotic cells (fragmented nuclei). Briefly, the dye was added to cultured cells at 10 μM for 30 min followed by fixing in a 3.7% PBS/paraform-

aldehyde for 10 min at room temperature. Cells were washed twice with PBS, stained for AIF protein (as described above), and mounted onto coverslips for visualization with a confocal microscopy (HeNe laser UV, 633 nm).

## RESULTS

To test whether NAD is transported into cells, NIH-3T3 cells were incubated for different lengths of time in Locke buffer containing 250  $\mu\text{M}$  [ $^{32}\text{P}$ ]NAD, and the reaction was stopped by aspiration of the buffer followed by a wash step with 1 ml of Locke buffer. When the amount of [ $^{32}\text{P}$ ]NAD was determined by scintillation counting, a significant amount was recovered from the cellular fraction (Fig. 1A). This amount corresponded to  $4.88 \pm 0.28$  fmol after 5 min and  $29.81 \pm 0.29$  fmol ( $\sim 24\%$  of total [ $^{32}\text{P}$ ]NAD present in the extracellular medium) after 1 h. We have previously shown a similar accumulation of NAADP into mast cells (17), and we tested the ability of NIH-3T3 cells to transport [ $^{32}\text{P}$ ]NAADP. When the experiment was repeated with 250  $\mu\text{M}$  [ $^{32}\text{P}$ ]NAADP,  $9.44 \pm 0.75$  fmol of NAADP were recovered after 5 min and  $38.07 \pm 0.57$  fmol after 1 h.

NAD uptake shows at least two phases with an initial rapid phase of transport followed by a prolonged phase of steady uptake up to at least an hour. NAD has previously been reported to bind to an extracellular P2Y purinergic receptor (P2Y<sub>11</sub> (30)). To identify whether a transport mechanism or a receptor mechanism was responsible for the observed NAD accumulation, experiments were performed whereby cells were treated with unlabeled NAD (100  $\mu\text{M}$ ) before or after treatment with 250  $\mu\text{M}$  [ $^{32}\text{P}$ ]NAD (Table 1). Cells were washed between treatments. Cells were also treated simultaneously with unlabeled and labeled NAD. The amount of NAD transported was reduced only in the co-treatment experiment indicating direct competition (Table 1). The lack of displacement when excess unlabeled NAD was added after the [ $^{32}\text{P}$ ]NAD indicates that a reversible binding site is not responsible, and the lack of inhibition by pre-treatment with unlabeled NAD rules out the presence of an irreversible binding site (Table 1). Furthermore, we can exclude that NAD is metabolized before transport, because all of the radioactivity remaining in the extracellular medium co-eluted with authentic NAD when assessed by HPLC (data not shown). We also assessed the fate of the transported [ $^{32}\text{P}$ ]NAD by extracting nucleotides and analyzing them by HPLC. We found that  $65.4 \pm 3.0\%$  of the transported radioactivity co-eluted with authentic NAD(H), whereas most of the remaining radioactivity eluted in a single peak co-eluting with NADP (Fig. 1B).

To further investigate transport we constructed a curve using a fixed concentration of labeled NAD (250  $\mu\text{M}$ ) and increasing concentration of unlabeled NAD, which allowed us to calculate an  $\text{IC}_{50}$  of  $66 \pm 29$   $\mu\text{M}$  (data not shown). Analysis of these data allowed us to construct a Michaelis-Menten plot (Fig. 1C). The apparent  $K_m$  of NAD transport was  $\sim 190$   $\mu\text{M}$  while the  $V_{\text{max}}$  was 429 pmol/well/10 min.

To determine whether the transport mechanism observed was the same as those previously described for NAADP and cADPR, the pharmacological properties of the mechanism were investigated (Table 2). In particular, NAADP transport has been shown to be  $\text{Na}^+$ - and  $\text{Ca}^{2+}$ -dependent and sensitive

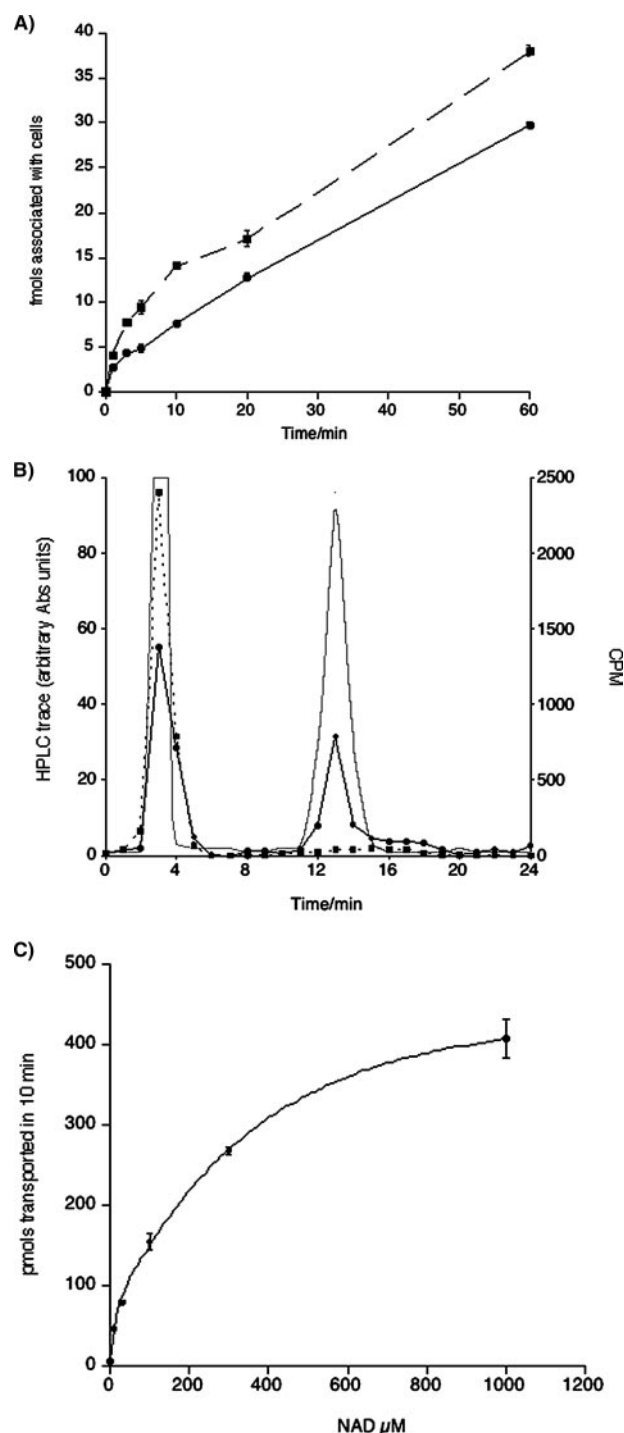


FIGURE 1. NAD transport in NIH-3T3 cells. A, time-dependent uptake of [ $^{32}\text{P}$ ]NAD (circles, solid line) and [ $^{32}\text{P}$ ]NAADP (squares, dashed line) in NIH-3T3 cells. Data presented as mean  $\pm$  S.E.,  $n = 8-12$ . B, HPLC analysis of transported nucleotides in NIH-3T3 cells. The gray line represents the HPLC trace for authentic standards (NAD, peak 3 min; NADP, peak 13 min). The other lines represent radioactivity remaining extracellularly (dashed line, squares) and recovered intracellularly (solid line, circles) after [ $^{32}\text{P}$ ]NAD incubation. C, kinetic plot of [ $^{32}\text{P}$ ]NAD uptake in NIH-3T3 cells. Data presented as mean  $\pm$  S.E.,  $n = 6-8$ .

to the nucleoside transport inhibitor dipyrindamole (DPR (17)), whereas cADPR transport has been shown to be  $\text{Na}^+$ -dependent and via one of three mechanisms: CD38 dimers (31), nucleoside transporters (18), or connexin hemichannels (10). As

## NAD Uptake

**TABLE 1**

**Transport of [<sup>32</sup>P]NAD in NIH-3T3 cells**

[<sup>32</sup>P]NAD was added at a concentration of 250 pM. In the sequential treatments, the first agent was washed away before addition of second agent. All treatments were for 10 min. Data are mean ± S.E. of respective controls; *n* = 4–8.

Treatment		Transport
		% of control
250 pM [ <sup>32</sup> P]NAD		100 ± 4.3
250 pM [ <sup>32</sup> P]NAD plus 100 μM NAD		49.2 ± 2.9
First treatment	Second treatment	
100 μM NAD	250 pM [ <sup>32</sup> P]NAD	102.7 ± 0.7
250 pM [ <sup>32</sup> P]NAD	100 μM NAD	112.1 ± 6.1

**TABLE 2**

**Pharmacology of [<sup>32</sup>P]NAD transport in NIH-3T3 cells**

Transport experiments were carried out for 10 minutes. Data are presented as the mean ± S.E., *n* = 6–15.

Treatment	Transport
	% of control
Control	100 ± 2.4
NMG Locke	21.1 ± 0.8
EGTA Locke	103.7 ± 1.9
NADP, 100 μM	87.7 ± 7.0
NAADP, 100 μM	78.1 ± 8.9
DPR, 100 μM	53.8 ± 5.4
Nitrobenzylthioinosine, 100 μM	169.6 ± 2.1
Adenosine, 100 μM	391.1 ± 14.5
Uridine, 100 μM	118.9 ± 1.9
Carboxelone, 100 μM	46.6 ± 0.2
Enoxelone, 100 μM	38.5 ± 1.4
Octanol, 1 mM	61.1 ± 2.8

NIH-3T3 cells are CD38-negative (32), we concentrated on the other two pathways. When NAD transport was performed in Locke buffer lacking NaCl or CaCl<sub>2</sub> (see “Experimental Procedures”), uptake was found to be significantly reduced in the absence of extracellular Na<sup>+</sup> (NMG Locke) but unaltered in the absence of extracellular Ca<sup>2+</sup> (EGTA Locke, Table 2). Because NAADP transport has previously been shown to be both Na<sup>+</sup>- and Ca<sup>2+</sup>-dependent, we investigated whether the insensitivity of NAD transport to extracellular Ca<sup>2+</sup> was a cell-specific or nucleotide-specific effect (17). When NAADP transport was carried out in the absence of extracellular Na<sup>+</sup> or Ca<sup>2+</sup>, uptake was significantly reduced in both buffers (NMG Locke: 44.8 ± 2.6% of control NAADP transport; EGTA Locke: 57.2 ± 3.5% of control NAADP transport). When NAD transport was performed in the presence of 100 μM of the nucleoside transport inhibitors DPR and nitrobenzylthioinosine or with the physiological substrates of these transporters (adenosine or uridine, 100 μM), the only treatment that inhibited transport was DPR (Table 2). Nitrobenzylthioinosine and uridine were without effect while adenosine significantly increased transport. These results suggest that nucleoside transporters are unlikely to mediate the uptake of NAD and that the effect of DPR is not related to the inhibition of these proteins. To evaluate the role of connexins, we used the inhibitors carboxelone (100 μM), enoxelone (100 μM), and octanol (1 mM). All three compounds were able to partially block NAD transport (Table 2).

Next, we decided to evaluate whether the NAD transport observed could have cellular consequences. To test this, we decided to take advantage of FK866, an inhibitor of the enzyme nicotinamide phosphoribosyltransferase (NMPRTase), which is a key enzyme in the NAD recycling pathway that mediates the

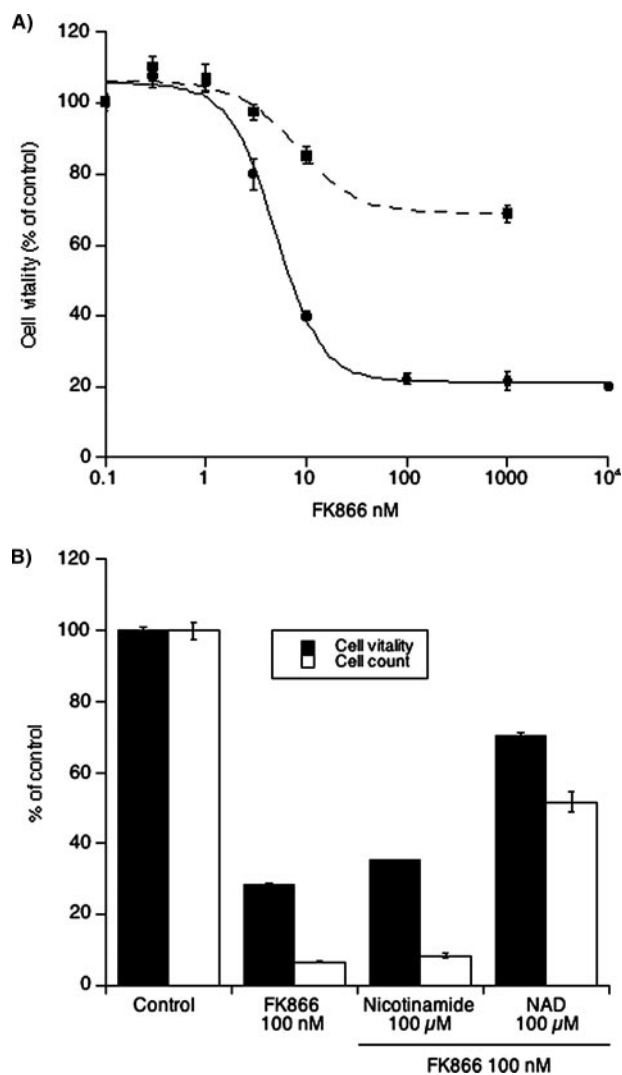


**FIGURE 2. FK866-induced NIH-3T3 cell death and rescue by extracellular NAD.** A, concentration response curve for the effect of FK866 on NIH-3T3 cell vitality after 48 h (squares, dashed line) or 72 h (circles, solid line) of treatment; *n* = 8–12. B, rescue of FK866-induced NIH-3T3 cell death by NAD. Data are presented for both cell vitality experiments (black bars) and cell counts (white bars); *n* = 4–12.

production of nicotinamide mononucleotide from dietary nicotinamide (niacin) (6, 25, 33). Because it induces cell death via the reduction of cellular NAD levels (25), it has now entered clinical trials for cancer treatment (2, 34).

In our hands, FK866 displayed an IC<sub>50</sub> of 4.90 ± 0.55 nM for cell vitality when cells were treated for 72 h with maximal effect at 100 nM (~78% cell death). FK866-induced cell death was time-dependent, with increasing levels of cell death between 24 (no apparent effect, data not shown) and 72 h (Fig. 2A). The IC<sub>50</sub> values for cell death at 48 or 72 h were similar (Fig. 2A). Extracellularly applied NAD (100 μM) reverted the effect of FK866 (Fig. 2B). Because the cell vitality assay we employed is based on a respiratory activity, which might be biased by changes in NAD levels, we also carried out cell counts to evaluate viability, and all results mirrored those obtained by MTT confirming the validity of the results obtained in the cell vitality assay (Fig. 2B). We then tested whether FK866-induced cell death and rescue by NAD could be explained simply by intra-

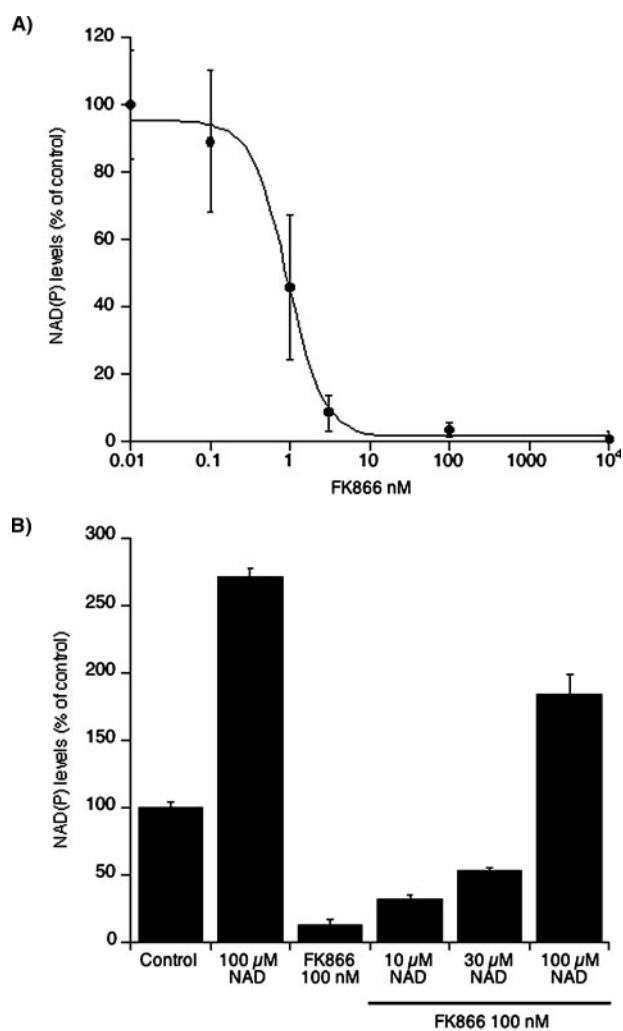


FIGURE 3. FK866-induced reduction in NAD(P) levels in NIH-3T3 cells and rescue by extracellular NAD. A, FK866-induced decrease in intracellular NAD(P) levels in NIH-3T3 cells after 24 h of treatment. Data presented as mean  $\pm$  S.E.,  $n = 9$ . B, rescue of FK866-induced decrease in intracellular NAD(P) levels in NIH-3T3 cells by extracellularly applied NAD;  $n = 9$ .

cellular NAD levels. To avoid artifacts due to cell death, we incubated cells with 100 nM FK866 for 24 h (an incubation time that yields no cell death) and evaluated total cellular NAD(P) levels with an NAD(P) cycling assay. Indeed, FK866 dose-dependently reduced cellular NAD(P) levels with an  $IC_{50}$  of  $926 \pm 130$  pM (Fig. 3A), whereas incubation with extracellular NAD replenished these levels in a concentration-dependent manner (Fig. 3B). Furthermore, cells that were treated with NAD alone displayed an increase in NAD(P) levels.

Alongside NIH-3T3 cells, we investigated whether NAD could be transported also in other cell types. Indeed, in SH-SH5Y (neuroblastoma) cells, NAD transport was present (total transport in 10 min,  $6.0 \pm 0.2$  fmol;  $n = 8$ ) and was sodium-dependent (NMG Locke:  $28.3 \pm 1.1\%$  of control transport;  $n = 4$ ) and calcium-independent (EGTA Locke:  $121 \pm 4.5\%$  of control transport;  $n = 4$ ). We also found NAD transport in HeLa (epithelial;  $8.2 \pm 0.3$  fmol/10 min), HaCaT (keratinocytes;  $2.2 \pm 0.2$  fmol/10 min), HMEC (endothelial;  $2.1 \pm 0.1$  fmol/10 min), and RAW 264.7 cells (macrophages;  $8.5 \pm 0.5$  fmol/10 min). Transport was significantly reduced in the absence of extracel-

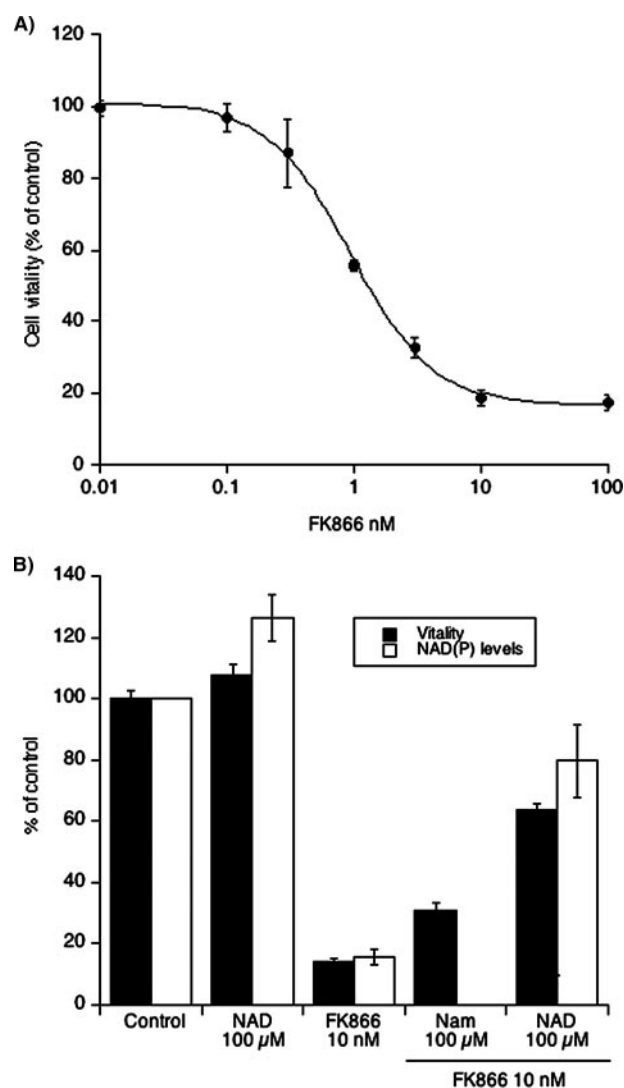


FIGURE 4. FK866-induced SH-SY5Y cell death and rescue by extracellular NAD. A, Concentration response curve for the effect of FK866 on SH-SY5Y cell vitality after 72 h of treatment;  $n = 8-16$ . B, rescue by extracellular NAD of FK866-induced SH-SY5Y cell death (black bars) and FK866-induced reduction of NAD(P) levels;  $n = 8-16$ . Nam, nicotinamide.

lular  $Na^+$  and partially inhibited in the presence of DPR in all cells tested. Although in RAW 264.7 cells, transport was insensitive to extracellular  $Ca^{2+}$ , in HMEC, HaCaT, and HeLa cells, NAD transport was inhibited by  $\sim 20\%$ , 50, and 80%, respectively, in EGTA Locke, perhaps suggesting diverse mechanisms or diverse regulation ( $n = 6$ ). NAD transport was not detected in K562 (leukemia) cells.

To confirm the data obtained with FK866 in NIH-3T3 cells, we repeated the experiments in SH-SY5Y cells. FK866 displayed a slightly higher  $IC_{50}$  than in NIH-3T3 cells in MTT experiments ( $0.93 \pm 0.06$  nM, Fig. 4A). This higher potency of FK866 in these cells prompted us to use 10 nM FK866, because this was the lowest concentration that could induce the maximal effect (Fig. 4). We tested the ability of extracellular NAD to rescue cells from FK866-induced cell death and intracellular NAD depletion and found near-identical results to those obtained for NIH-3T3 cells (Fig. 4B), other than a slightly lower rescue by 100 μM NAD, which, along with the higher potency of

**TABLE 3****Rescue of FK866-induced cell death by intermediates in the NAD-recycling pathway**

Cells were treated for 72 h with FK866 (100 nM for NIH-3T3 cells and 10 nM for SH-SY5Y cells) in the presence or absence of various intermediates in the NAD-recycling pathway. Cell vitality was assessed after 72 h by MTT. Results expressed as % of control,  $n = 8-16$ .

Treatment	Cell vitality	
	% of control	
	NIH-3T3	SH-SY5Y
Control	100 ± 2.5	100 ± 2.3
FK866	29.8 ± 0.9	25.2 ± 2.4
FK866 plus nicotinic acid, 100 μM	29.9 ± 0.6	20.3 ± 0.4
FK866 plus nicotinamide, 100 μM	35.2 ± 0.6	23.9 ± 0.6
FK866 plus nicotinic acid mononucleotide, 100 μM	77.2 ± 1.9	69.8 ± 5.0
FK866 plus nicotinamide mononucleotide, 100 μM	77.3 ± 2.7	70.2 ± 4.6
FK866 plus NAD, 100 μM	85.4 ± 2.5	78.6 ± 1.3

FK866 perhaps due to a higher NAD turnover in these cells. Similar FK866-induced cell death and rescue by NAD was also observed in HeLa cells.<sup>3</sup> To investigate whether cell death and subsequent rescue were due to the specific inhibition of NMPRTase and reduction of NAD levels, we performed rescue experiments in NIH-3T3 and SH-SY5Y cells using compounds that enter the recycling pathway either before or after the step catalyzed by NMPRTase (Table 3). As might be expected, neither nicotinamide nor nicotinic acid was able to rescue cells, because they are the substrates for NMPRTase. However, these data are in contrast to the work of Hasmann and Schemainda (25) who reported rescue with both nicotinic acid and nicotinamide. On the contrary, nicotinamide mononucleotide and nicotinic acid mononucleotide, which feed into the recycling pathway after NMPRTase, were able to rescue cells as efficiently as NAD itself (Table 3) suggesting that the effects of FK866 are specific.

As described above, in our cellular models FK866 caused cell death in a peculiar delayed fashion compared with the drop of NAD(P) levels. Consequently, we sought to characterize the type of death induced by FK866 in SH-SY5Y cells by evaluating markers of apoptosis and autophagy. We first assayed the caspase-dependent pathway of apoptosis by evaluating caspase 3 cleavage. Indeed, this protease is invariably recruited as an effector of the apoptotic caspase machinery, because it is cleaved to enzymatically active products by the upstream caspases (caspase 9–10 (35) to dismantle the dying cell. Surprisingly, the caspase 3 activation fragment (p11) was not detected in FK866-treated cells (10 nM) even after 72 h of treatment, as assessed by Western blot with a p11-specific antibody (data not shown). On the other hand, apoptosis may rely on the activation of mitochondria to release pro-apoptotic mediators such as cytochrome *c* (*cyt-c*) and the apoptosis-inducing factor (AIF) (36, 37). To evaluate this pathway, we studied the cellular distribution of *cyt-c* and AIF by immunodetection with confocal microscopy. This approach demonstrated that, in the majority of the cells, neither *cyt-c* nor AIF were released from the mitochondria, thereby excluding the engagement of apoptotic death (Fig. 5) with the exception of rare populations of cells sporadically detected. Further proof of this came from vital DNA staining

<sup>3</sup> A. A. Grolla and R. A. Billington, unpublished observation.

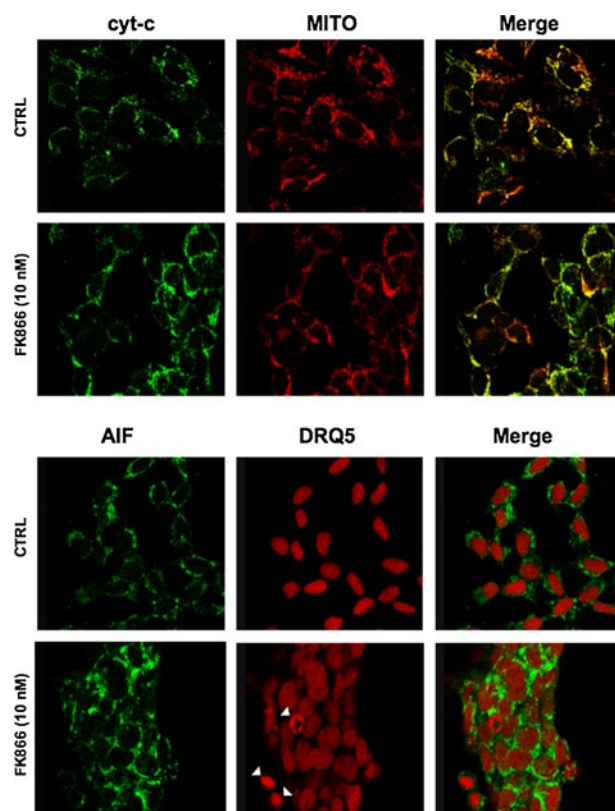


**FIGURE 5. FK866 does not induce apoptosis in SH-SY5Y cells.** Cells were co-stained with a *cyt-c* antibody and MitoTracker or with an AIF antibody and the nuclear marker DRQ5. Cells were treated for 48 h as indicated. Results are indicative of four cultures.

with the fluorescent DRQ5 (used as counterstain for AIF nuclear localization), because typical apoptotic fragmented nuclei were detected in only a very small number of FK866-treated cells (Fig. 5). Given the lack of correlation between the intense cytotoxic effect induced by FK866 and the exiguity of the apoptosis detected, we investigated the possibility that FK866 could induce autophagy. Indeed, the length of time required to achieve cell death, abnormally long for a canonical apoptosis, and the energetic relevance of an impaired NAD biosynthesis may be indicative of a metabolic crisis pushing the cell to a compensatory behavior such as autophagy. To address this hypothesis, we studied, by confocal microscopy, the formation of autophagic vesicles (autophagosomes and autophagolysosomes), upon FK866-induced NAD depletion. These sub-cellular membranous structures, originating from the coalescence of small vesicles with lysosomes, are characteristically endowed with the microtubule-associated protein light chain 3 (LC3)-specific marker (38). Indeed LC3, which is mainly cytosolic and diffuse in healthy cells, is conjugated to phosphatidylethanolamine upon induction of autophagy and targeted to autophagosomes, thus allowing their detection. Because the commercially available anti-LC3 antibodies are not reliable for immunofluorescence studies, we transiently overexpressed EYFP-tagged LC3 in neuroblastoma cells that were treated with FK866 for different times (Fig. 6). In such conditions we were able to track the generation of LC3-positive autophagic vacuoles in FK866-treated cells, but not in control cells, already after 24-h treatment (Fig. 6). Validating the autophagic nature of this

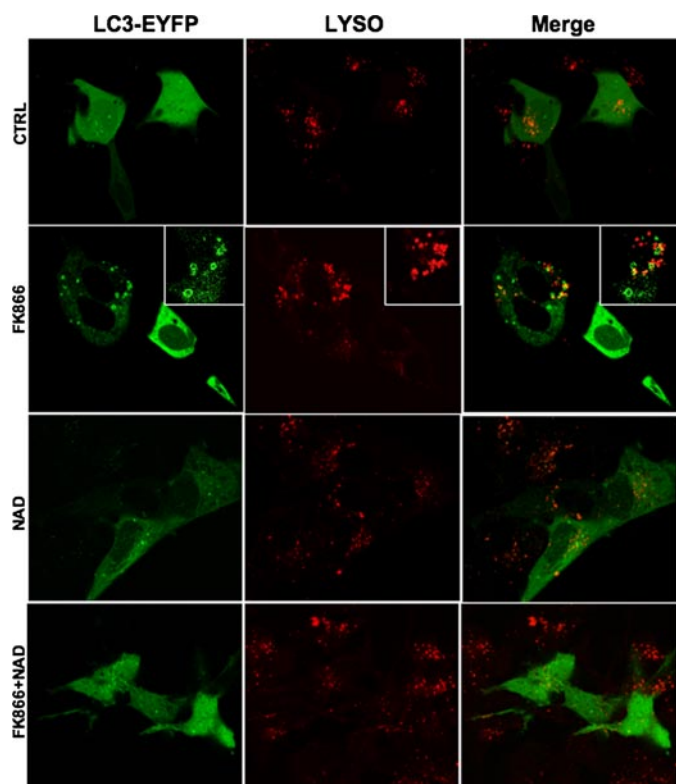


FIGURE 6. **FK866-induced autophagy in SH-SY5Y cells.** Cells were transiently transfected with LC3-EYFP and stained with LysoTracker and treated with FK866 (10 nM) and NAD (100  $\mu$ M) either alone or together for 36 h. Results are indicative of five cultures.

LC3 vesicle, the vital staining of lysosomes (LysoTracker) allowed us to detect the presence of these organelles in the LC3-positive structures (Fig. 6). In line with data from the cell count and MTT assays, the percentage of cells presenting the LC3-positive vesicles reached  $44.3 \pm 5.1\%$  after 36-h treatment with 10 nM FK866. More importantly, repletion of the NAD levels with 100  $\mu$ M extracellular NAD was able to revert the autophagic phenotype almost entirely.

## DISCUSSION

There has been a recent resurgence in interest in NAD(P), because it is becoming clear that, in addition to its role in basic metabolism, these nucleotides play an important role in signal transduction (4). In the present report, we have investigated whether low concentrations of NAD could be transported into the cytoplasm from the extracellular space and could then enter the cellular NAD(H) pool. To accomplish this, we first used radiolabeled NAD to monitor uptake in various cell lines. Six out of seven cell lines tested were able to accumulate different amounts of NAD. The only cell line unable to accumulate NAD was K562, the cells of which grow in suspension. Interestingly, we have not found NAADP transport in either Jurkat or HL-60 cell lines growing in suspension.<sup>4</sup> Although these data suggest that NAD transport is not ubiquitous, they may suggest that it is a widespread mechanism.

Accumulation was not due to extracellular membrane binding (for example to purinergic receptors) as the radioactivity

could not be displaced. These data, therefore, strongly agree with circumstantial evidence by others suggesting that extracellular NAD can enter cells (10, 12–15). NAD uptake has been previously shown at millimolar concentrations, and it has been proposed that connexin hemichannels (e.g. Cx43) might mediate bidirectional NAD transport down a concentration gradient. In our hands, NAD transport occurred at low concentrations of NAD (e.g. 250 pM, far lower than the intracellular concentration), which suggest that NAD is moving up its concentration gradient. NAD was not degraded extracellularly, and the majority of the radioactivity transported remained as NAD. A proportion of the transported NAD was found to have been metabolized intracellularly, because presumably it had joined the pool of intracellular NAD. A pharmacological profile of transport to elucidate this showed that hemichannel inhibitors were able to partially inhibit NAD transport, whereas adenosine and uridine, competitors for nucleoside transporters, were devoid of any inhibitory effect. Further evidence against a role for nucleoside transporters was brought by a lack of effect of nitrobenzylthioinosine. Yet, DPR, a different inhibitor of nucleoside transporters, was partially effective at inhibiting transport. These pharmacological data collectively might suggest that more than one protein family contributes to transport and that hemichannels play a major role, as proposed by others in different settings (9, 12). Yet, in our opinion, a number of issues suggest that canonical hemichannels alone cannot explain the results presented here: (i) the removal of extracellular  $\text{Ca}^{2+}$ , which should open hemichannels, has no effect on NAD uptake in NIH-3T3, SH-SY5Y, or RAW 264.7 cells, and in HaCaT, HMEC, and HeLa cells, the removal of extracellular  $\text{Ca}^{2+}$  reduced transport; (ii) given the large difference between the intracellular and extracellular concentrations of NAD in our experiments, hemichannels would be expected to mediate NAD efflux and not influx; (iii) the removal of extracellular  $\text{Na}^+$ , which almost completely inhibits NAD uptake, has not been shown to regulate the gating of hemichannels; and (iv) the time course of NAD uptake would appear to indicate that it is a constitutive mechanism that is incompatible with a canonical channel mechanism. Last, given the high concentrations of pharmacological inhibitors required to obtain effects, we cannot exclude that other related protein families might be affected by these.

Transport of the three related nucleotides NAD(H), cADPR, and NAADP from the extracellular space has now been demonstrated. Several protein families have been shown to transport these nucleotides, including CD38, nucleoside transporters, and connexin hemichannels (9, 10, 12, 17, 18, 31). It is interesting to note that certain similarities exist in the pharmacology of these transport systems such as sodium dependence and inhibition by selected inhibitors of both nucleoside transporters and connexin hemichannels. However, certain differences, such as the sensitivity of NAADP transport to extracellular calcium and discrepancies in the effects of some of the nucleoside transport substrates/inhibitors may point to diverse mechanisms, redundant mechanisms, or differential regulation of nucleotide transport (17). Furthermore, it is not clear how or if the extracellular concentration of nucleotides might play a role in the recruitment of pharmacologically distinct uptake

<sup>4</sup> R. A. Billington and A. A. Grolla, unpublished observation.

mechanisms. Identification of the molecular nature of the transporter(s) will be required to resolve these questions and to identify which nucleotide(s)/nucleotide derivative(s) are the physiologically relevant substrates in diverse cell types under diverse physiological or pathological conditions and in an *in vivo* setting.

Independently of the nature of the transporter, the magnitude of transport prompted us to speculate that the transport might be physiologically relevant. Indeed, there is evidence that NAD is present extracellularly, for example in plasma (23), and our data have confirmed this (concentrations in calf and horse serum were  $1.8 \pm 0.8 \mu\text{M}$  and  $1.6 \pm 0.5 \mu\text{M}$ , respectively;  $n = 6$ ). It is interesting to note that positive cooperativity of NAD transport was observed in this concentration range (data not shown). To test the physiological relevance, we inhibited the NAD recycling pathway using the NMPRTase inhibitor FK866 (25). Treatment of cells for 24 h with nanomolar concentrations of this inhibitor resulted in a significant drop in intracellular NAD(P) levels, demonstrating a high turnover of pyridine nucleotides, at least in cultured cells in line with previous reports (25). Extracellular application of NAD was able to counteract this drop and replenish intracellular levels in all three cell types examined (NIH-3T3, SH-SY5Y, and HeLa). Interestingly, incubation of cells with NAD alone induced a significant increase in intracellular NAD levels, suggesting that uptake of pyridine nucleotides is constitutive and participates in cellular NAD homeostasis. In parallel, experiments performed on cell vitality showed that NAD uptake could functionally replenish NAD levels, because it could save cells from FK866-induced cell death. To rescue cells and replete NAD levels, micromolar concentrations were required, but this is not in contradiction with transport experiments as: (i) intracellular concentrations of NAD are estimated to be in the high micromolar or the millimolar range (25); (ii) abolition of NMPRTase activity does not allow recycling; and (iii) experiments measuring cell vitality or NAD(P) levels after treatment with FK866 suggest a high turnover of NAD(P). Our conclusion that NAD transport is a valid replenishment pathway is supported by previous observation that extracellular NAD can rescue cardiomyocytes (15) and astrocytes (12) from poly(ADP-ribose) polymerase-mediated cell death and can activate sirtuins (15). Along the same lines, it is interesting to note that CD38 knock-out mice, which are impaired in their ability to degrade extracellular NAD, display higher endogenous SIRT1 activity (16).

Last, we were intrigued by the discrepancy in the latency between FK866-induced NAD depletion and cell death, and decided to investigate the mechanisms leading to cell death. We found that cells did not enter into an apoptotic program but instead entered into autophagy. Once again, even from a mechanistic viewpoint, extracellular NAD could counteract the effects of intracellular NAD depletion.

### REFERENCES

- Ziegler, M. (2000) *Eur. J. Biochem.* **267**, 1550–1564
- Khan, J. A., Forouhar, F., Tao, X., and Tong, L. (2007) *Expert Opin. Ther. Targets* **11**, 695–705
- Belenky, P., Bogan, K. L., and Brenner, C. (2007) *Trends Biochem. Sci.* **32**, 12–19
- Berger, F., Ramirez-Hernandez, M. H., and Ziegler, M. (2004) *Trends Biochem. Sci.* **29**, 111–118
- Lee, H. C. (2006) *Mol. Med.* **12**, 317–323
- Magni, G., Amici, A., Emanuelli, M., Orsomando, G., Raffaelli, N., and Ruggieri, S. (2004) *Cell Mol. Life Sci.* **61**, 19–34
- Bieganowski, P., and Brenner, C. (2004) *Cell* **117**, 495–502
- Billington, R. A., Bruzzone, S., De Flora, A., Genazzani, A. A., Koch-Nolte, F., Ziegler, M., and Zocchi, E. (2006) *Mol. Med.* **12**, 324–327
- Bruzzone, S., Guida, L., Zocchi, E., Franco, L., and De Flora, A. (2001) *FASEB J.* **15**, 10–12
- Bruzzone, S., Franco, L., Guida, L., Zocchi, E., Contini, P., Bisso, A., Usai, C., and De Flora, A. (2001) *J. Biol. Chem.* **276**, 48300–48308
- Smyth, L. M., Bobalova, J., Mendoza, M. G., Lew, C., and Mutafova-Yambolieva, V. N. (2004) *J. Biol. Chem.* **279**, 48893–48903
- Ying, W., Garnier, P., and Swanson, R. A. (2003) *Biochem. Biophys. Res. Commun.* **308**, 809–813
- Zocchi, E., Usai, C., Guida, L., Franco, L., Bruzzone, S., Passalacqua, M., and De Flora, A. (1999) *FASEB J.* **13**, 273–283
- Zhu, K., Swanson, R. A., and Ying, W. (2005) *Neuroreport* **16**, 1209–1212
- Pillai, J. B., Isbatan, A., Imai, S., and Gupta, M. P. (2005) *J. Biol. Chem.* **280**, 43121–43130
- Barbosa, M. T., Soares, S. M., Novak, C. M., Sinclair, D., Levine, J. A., Aksoy, P., and Chini, E. N. (2007) *FASEB J.* **21**, 3629–3639
- Billington, R. A., Bellomo, E. A., Floriddia, E. M., Erriquez, J., Distasi, C., and Genazzani, A. A. (2006) *FASEB J.* **20**, 521–523
- Guida, L., Bruzzone, S., Sturla, L., Franco, L., Zocchi, E., and De Flora, A. (2002) *J. Biol. Chem.* **277**, 47097–47105
- Guida, L., Franco, L., Bruzzone, S., Sturla, L., Zocchi, E., Basile, G., Usai, C., and De Flora, A. (2004) *J. Biol. Chem.* **270**, 22066–22075
- Podesta, M., Benvenuto, F., Pitto, A., Figari, O., Bacigalupo, A., Bruzzone, S., Guida, L., Franco, L., Paleari, L., Bodrato, N., Usai, C., De Flora, A., and Zocchi, E. (2004) *J. Biol. Chem.* **280**, 5343–5349
- Heidemann, A. C., Schipke, C. G., and Kettenmann, H. (2005) *J. Biol. Chem.* **280**, 35630–35640
- Revollo, J. R., Grimm, A. A., and Imai, S. (2007) *Curr. Opin. Gastroenterol.* **23**, 164–170
- O'Reilly, T., and Niven, D. F. (2003) *Can. J. Vet. Res.* **67**, 229–231
- Araki, T., Sasaki, Y., and Milbrandt, J. (2004) *Science* **305**, 1010–1013
- Hasmann, M., and Schemainda, I. (2003) *Cancer Res.* **63**, 7436–7442
- Billington, R. A., and Genazzani, A. A. (2000) *Biochem. Biophys. Res. Commun.* **276**, 112–116
- Morgan, A., Churchill, G., Masgrau, R., Ruas, M., Davis, L., Billington, R., Patel, S., Yamasaki, M., Thomas, J., Genazzani, A., and Galione, A. (2005) in *Methods in Calcium Signalling* (Putney, J. J., ed), 2nd Ed., pp. 265–334, CRC Press, Boca Raton
- Gasser, A., Bruhn, S., and Guse, A. H. (2006) *J. Biol. Chem.* **281**, 16906–16913
- Biedermann, E., Hasmann, M., Loser, R., Rattel, B., Reiter, F., Schein, B., Seibel, K., and Vogt, K. (June 7, 2005) U. S. Patent 6, **903**, 118
- Moreschi, I., Bruzzone, S., Nicholas, R. A., Fruscione, F., Sturla, L., Benvenuto, F., Usai, C., Meis, S., Kassack, M. U., Zocchi, E., and De Flora, A. (2006) *J. Biol. Chem.* **281**, 31419–31429
- Franco, L., Guida, L., Bruzzone, S., Zocchi, E., Usai, C., and De Flora, A. (1998) *Faseb. J.* **12**, 1507–1520
- Zocchi, E., Daga, A., Usai, C., Franco, L., Guida, L., Bruzzone, S., Costa, A., Marchetti, C., and De Flora, A. (1998) *J. Biol. Chem.* **273**, 8017–8024
- Khan, J. A., Tao, X., and Tong, L. (2006) *Nat. Struct. Mol. Biol.* **13**, 582–588
- Holen, K., Saltz, L. B., Hollywood, E., Burk, K., and Hanauke, A. R. (2008) *Invest. New Drugs.* **26**, 45–51
- Cohen, G. M. (1997) *Biochem. J.* **326**, 1–16
- Cai, J., Yang, J., and Jones, D. P. (1998) *Biochim. Biophys. Acta* **1366**, 139–149
- Susin, S. A., Lorenzo, H. K., Zamzami, N., Marzo, I., Snow, B. E., Brothers, G. M., Mangion, J., Jacotot, E., Costantini, P., Loeffler, M., Larochette, N., Goodlett, D. R., Aebersold, R., Siderovski, D. P., Penninger, J. M., and Kroemer, G. (1999) *Nature* **397**, 441–446
- Tanida, I., Minematsu-Ikeguchi, N., Ueno, T., and Kominami, E. (2005) *Autophagy* **1**, 84–91

## Characterization of NAD Uptake in Mammalian Cells

Richard A. Billington, Cristina Travelli, Emanuela Ercolano, Ubaldina Galli, Cintia Blasi Roman, Ambra A. Grolla, Pier Luigi Canonico, Fabrizio Condorelli and Armando A. Genazzani

*J. Biol. Chem.* 2008, 283:6367-6374.

doi: 10.1074/jbc.M706204200 originally published online January 7, 2008

---

Access the most updated version of this article at doi: [10.1074/jbc.M706204200](https://doi.org/10.1074/jbc.M706204200)

### Alerts:

- [When this article is cited](#)
- [When a correction for this article is posted](#)

[Click here](#) to choose from all of JBC's e-mail alerts

This article cites 36 references, 16 of which can be accessed free at <http://www.jbc.org/content/283/10/6367.full.html#ref-list-1>